

Analytical Molecular Surface Calculation

BY MICHAEL L. CONNOLLY

Department of Molecular Biology, Research Institute of Scripps Clinic, 10666 North Torrey Pines Road, La Jolla, California 92037, USA

(Received 3 March 1983; accepted 27 May 1983)

Abstract

A computer algorithm is presented for calculating the part of the van der Waals surface of a molecule that is accessible to solvent. The solvent molecule is modeled by a sphere. This sphere is, in effect, rolled over the molecule to generate a smooth outer-surface contour. This surface contour is made up of pieces of spheres and tori that join at circular arcs. The spheres, tori and arcs are defined by analytical expressions in terms of the atomic coordinates, van der Waals radii and the probe radius. The area of each surface piece may be calculated analytically and the surface may be displayed on either vector or raster computer-graphics systems. These methods are useful for studying the structure and interactions of proteins and nucleic acids.

Introduction

In order to study the structure and function of proteins and nucleic acids, it is desirable to define precisely the outer surface of a macromolecule. It is this part of the molecule that binds ligands and other macromolecules. For small molecules the van der Waals surface gives a good representation of the outer surface and overall shape. But, for large molecules, most of the van der Waals surface is buried in the interior. Some other method is required to define the outer surface of a macromolecule.

A suitable definition has been presented by Richards (1977). This molecular surface consists of two parts: the contact surface and the reentrant surface. The contact surface is that part of the van der Waals surface of the atoms that is accessible to a probe sphere representing a solvent molecule. The reentrant surface comes from the inward-facing surface of the probe sphere when it is simultaneously in contact with more than one atom. Richards, however, has not presented a method for calculating this surface.

This surface definition is an improvement over the earlier solvent-accessible surface of Lee & Richards (1971), which was displaced outward from the true surface of the molecule by a distance equal to the probe radius. This earlier surface definition has been

implemented by several computer algorithms (Lee & Richards, 1971; Richmond & Richards, 1978; Alden & Kim, 1979). The two surfaces are compared to each other and to the van der Waals surface in Fig. 1.

There have been several attempts to implement Richards's (1977) definition. Finney (1978) has calculated molecular area, where the outer surface of the protein is represented by a polyhedron with flat faces, roughly approximating Richards's surface. Greer & Bush (1978) have developed an algorithm where a rectangular grid of probe spheres is dropped on one face of a protein. Points selected from the bottoms of these spheres approximate the surface of that face of the protein.

The author has presented an algorithm which places dots over the solvent-accessible molecular surface (Connolly, 1981*a, b*). In this method, a probe sphere is placed tangent to each atom, each pair of neighboring atoms and each triple of neighboring atoms. When the probe is free from collisions with other atoms, points lying on the inward-facing surface of the probe sphere are chosen to become part of the molecular surface. The probe is moved around each atom and pair of atoms in angular increments, so this is a numerical and not an analytical algorithm. The dot surface numerical algorithm is described in more detail in Appendix II, and its scientific applications are discussed elsewhere (Connolly, 1983*a*). A dot surface for insulin (Dodson, Dodson, Hodgkin & Reynolds, 1979) is shown in Fig. 2.

An analytical method for calculating Richards's molecular surface is presented in detail below. The output of this computer algorithm consists of a set of curved regions of spheres and tori, joined together at

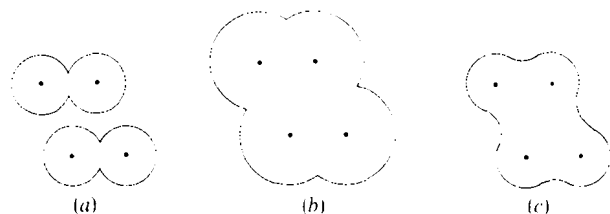


Fig. 1. Surface comparison. (a) van der Waals surface. (b) Lee & Richards's (1971) solvent-accessible surface. (c) Richards's (1977) molecular surface.

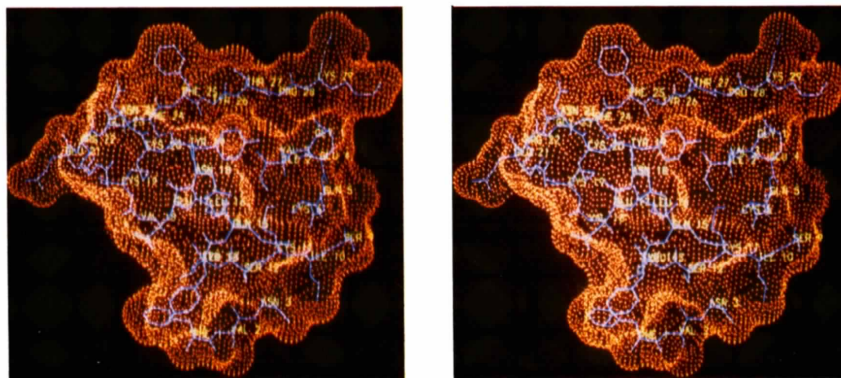
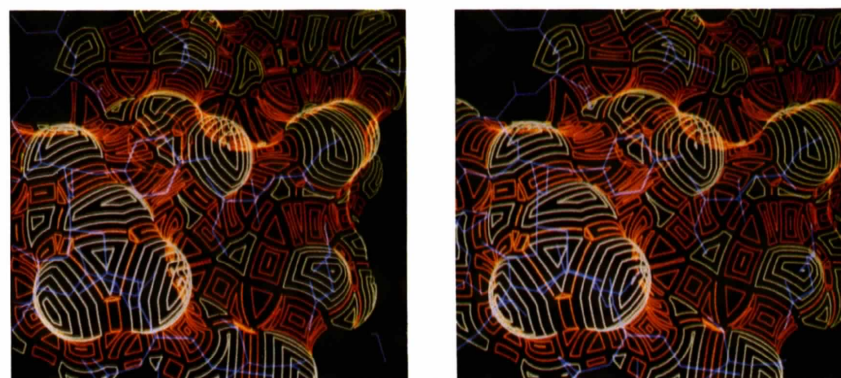
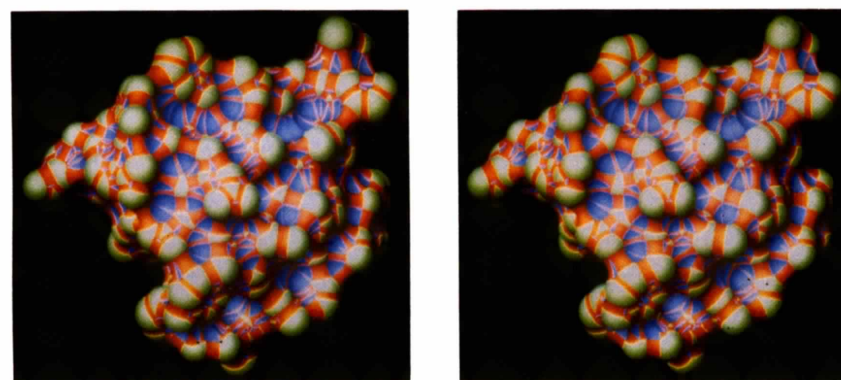


Fig. 2. Stereo pair of insulin dot surface. Amino-acid residues are labeled at α -carbon positions.



(a)



(b)

Fig. 3. Analytical molecular surface of insulin. Two stereo pairs. (a) Vector graphics system representation. Close-up of surface, with same viewpoint as Fig. 2. Each face is drawn as concentric curved polygons. Green: contact surface. Red: reentrant surface. (b) Raster graphics system representation. Green: convex surface. Red: saddle-shaped surface. Blue: concave surface.

circular arcs. Two applications of this analytically defined surface are presented. The first application shows how molecular areas may be computed, and the second shows how the surface may be visualized on a vector computer graphics system.

Surface creation

The rolling of a probe sphere over a molecule is best understood in terms of translational degrees of freedom. If the probe is not in contact with the molecule, it will have three degrees of freedom. It loses one degree of freedom for each atom that it touches. There are then three cases for the number of atoms that a probe sphere may simultaneously touch (Table 1).

A differently shaped piece of surface is generated for each of these three cases (Fig. 3). Each piece is defined by the sphere or torus it lies on and a boundary contour. Each sphere is defined by a center and a radius. Each torus is defined by a center, two radii and an axial vector. The boundary of each piece of surface is defined by a set of circular arcs, each arc being defined by its center, radius, plane and end points.

These pieces of surface form a connected network covering the molecule. Because this network is analogous to a polyhedron, except for the fact that it is curved, we call each piece of surface a face. The faces are joined together at common boundary arcs, sometimes referred to as edges. The arcs meet at points called vertices. The join between two faces is smooth, in the sense that there is a well-defined tangent plane at each point of the arc joining the faces. This is in contrast to the van der Waals surface of a molecule, where there are sharp crevices where atoms intersect.

The equations defining the surface are given in Table 2 and the data structure of the computer representation of the surface is diagrammed in Fig. 4. Below, I discuss the details of the computer algorithm. The derivations of the equations are presented in Appendix I.

The basic idea of the computer algorithm is to bootstrap up from probe-sphere positions having no translational degrees of freedom. These discrete positions form the starting and stopping points of the trajectories of the probe when it has one degree of freedom. These trajectories, in turn, form the border of the rolling of a probe with two degrees of freedom.

Torus construction

The construction of concave and saddle faces requires that a torus be calculated for each pair of neighboring atoms, i and j . Two atoms are defined to be neighbors if the distance between their atom centers is less than the sum of their van der Waals radii plus the probe diameter. This ensures that they will be close enough to be bridged by a probe sphere. In order to avoid duplication of tori, i is chosen to be less than j .

Table 1. Three shapes of surface pieces

Atoms touching probe	Degrees of freedom	Surface	Shape	Boundary
1	2	Sphere	Convex	Cycles of convex arcs
2	1	Torus	Saddle	Convex and concave arcs
3	0	Sphere	Concave	Three concave arcs

Table 2. Surface definition equations

Variable name	Value
Atomic coordinates	$\mathbf{a}_i, \mathbf{a}_j, \mathbf{a}_k, \dots$ (input)
van der Waals radii	r_i, r_j, r_k, \dots (input)
Probe radius	r_p (input)
Inter-atomic distance	$d_{ij} = \mathbf{a}_j - \mathbf{a}_i $
Torus axis unit vector	$\mathbf{u}_{ij} = (\mathbf{a}_j - \mathbf{a}_i) / d_{ij}$
Torus center	$\mathbf{t}_{ij} = \frac{1}{2}(\mathbf{a}_i + \mathbf{a}_j) + \frac{1}{2}(\mathbf{a}_j - \mathbf{a}_i) \times [(r_i + r_p)^2 - (r_j + r_p)^2] / d_{ij}^2$
Torus radius	$r_{ij} = \frac{1}{2}[(r_i + r_j + 2r_p)^2 - d_{ij}^2]^{1/2} \times [d_{ij}^2 - (r_i - r_j)^2]^{1/2} / d_{ij}$
Base triangle angle	$\omega_{ijk} = \arccos(\mathbf{u}_{ij} \cdot \mathbf{u}_{ik})$
Base plane normal vector	$\mathbf{u}_{ijk} = \mathbf{u}_{ij} \times \mathbf{u}_{ik} / \sin \omega_{ijk}$
Torus-basepoint unit vector	$\mathbf{u}_{ib} = \mathbf{u}_{ijk} \times \mathbf{u}_{ij}$
Base point	$\mathbf{b}_{ijk} = \mathbf{t}_{ij} + \mathbf{u}_{ib} [\mathbf{u}_{ik} \cdot (\mathbf{t}_{ik} - \mathbf{t}_{ij}) \times (\sin \omega_{ijk})^{-1}]$
Probe height	$h_{ijk} = [(r_i + r_p)^2 - \mathbf{b}_{ijk} - \mathbf{a}_i ^2]^{1/2}$
Probe position	$\mathbf{p}_{ijk} = \mathbf{b}_{ijk} \pm h_{ijk} \mathbf{u}_{ijk}$
Vertex	$\mathbf{v}_{pi} = (r_i \mathbf{p}_{ijk} + r_p \mathbf{a}_i) / (r_i + r_p)$
Contact circle center	$\mathbf{c}_{ij} = (r_i \mathbf{t}_{ij} + r_p \mathbf{a}_i) / (r_i + r_p)$
Contact circle radius	$r_c = r_{ij} r_i / (r_i + r_p)$
Contact circle displacement	$d_c = \mathbf{u}_{ij} \cdot (\mathbf{c}_{ij} - \mathbf{a}_i)$
Concave arc plane normal vector	$\mathbf{n}_{ijk} = (\mathbf{p}_{ijk} - \mathbf{t}_{ij}) \times \mathbf{u}_{ij} / r_{ij}$
Concave triangle angle	$\beta_i = \arccos(\mathbf{n}_{ijk} \cdot \mathbf{n}_{ikj})$
Convex face angle	$\alpha_i = \pi - \beta_i$
Saddle wrap angle	$\varphi_s = \arccos(\mathbf{n}_{ijk} \cdot \mathbf{n}_{ijl})$ when $\mathbf{n}_{ijk} \times \mathbf{n}_{ijl} \cdot \mathbf{u}_{ij} \geq 0$ $= -\arccos(\mathbf{n}_{ijk} \cdot \mathbf{n}_{ijl}) + 2\pi$ when $\mathbf{n}_{ijk} \times \mathbf{n}_{ijl} \cdot \mathbf{u}_{ij} < 0$
Saddle width angle	$\theta_{si} = \arctan(d_c / r_c)$
Euler characteristic	$\chi = 2 - \text{number of cycles}$

As the probe is rolled around atoms i and j , its center traces out a circle and its surface traces out the volume of a torus. The inward-facing arc that connects the two points of contact on the probe sphere sweeps out an area that is the inner face of the torus. It is neither convex nor concave, but saddle shaped (Fig. 5). We call the circle traced by the probe center the torus central circle, its center the torus center, its radius the torus radius, and the plane that it lies in the torus plane. The equations for the torus center and radius are given in Table 2. The line through the atom centers

is referred to as either the torus axis or the inter-atomic axis. The torus plane is perpendicular to the torus axis and bisects the torus.

The expression for the torus radius given in Table 2 contains two square roots. The quantity under the first square root will be negative if the two atoms are too far apart to be bridged by a probe sphere. The quantity under the second square root can be negative only in the situation where one atom is inside the other, a situation that is not chemically realistic. No torus is constructed in either of these situations.

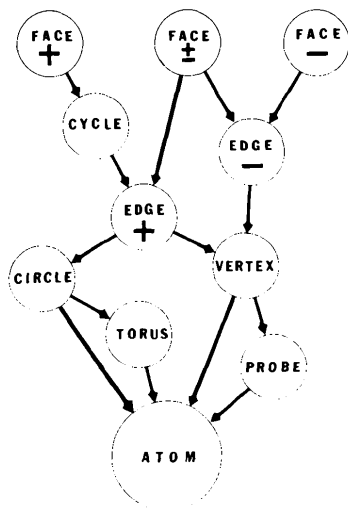


Fig. 4. Data structure of surface. The plus, minus and plus-minus signs mean convex, concave and saddle-shaped, respectively. The arrows indicate pointers. For example, an entry in the array of saddle faces contains the integer indices of elements in the convex-edge and concave-edge arrays. Entries in face, cycle and edge arrays consist solely of such pointers. Entries in circle, torus, vertex and probe arrays also contain real-valued geometric information, such as centers, radii and axes. The atom array contains only real-valued geometric information, *i.e.* atomic coordinates and van der Waals radii.

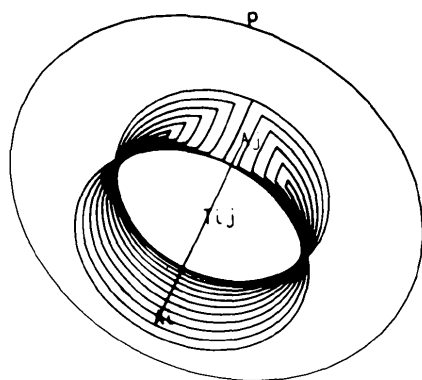


Fig. 5. Torus construction. The torus central circle (probe trajectory) and inward-facing part of the torus surface are shown. The torus center and atom centers are labeled.

Probe placement

Along the torus central circle of atoms i and j , there may be points where a probe sphere may be placed so that it is also tangent to another atom. These other atoms must be mutual neighbors of atoms i and j , that is, each must be a neighbor of atom i and a neighbor of atom j . There are two possible probe placements for each such atom k , one on each side of the plane passing through the three atom centers.

The midpoint of the two possible probe positions lies on the plane passing through the three atom centers and is called the base point, because it sits at the base of the altitudes to the probe centers (Fig. 6). The length of the altitude is called the probe height. Equations for the base point, probe height and probe positions are given in Table 2. If the three atoms are collinear, the denominator in the expression for the base point will be zero and there will be no probe placement.

There are two cases where the quantity under the square root in the expression for the probe height will be negative and there will be no probe placement for atom k . The first case occurs when atom k is too far away for the probe to collide with it as the probe rolls around atoms i and j . If this happens with every mutual neighbor of atoms i and j , or if there are no mutual neighbors of atoms i and j , then this torus is called a free torus, because the probe is free to roll all the way around the pair of atoms, without collision. The second case occurs when atom k is located between atoms i and j so that the probe always experiences van der Waals overlap with atom k while rolling around atoms i and j . If this happens with any mutual neighbor of atoms i and j , then this torus is called a completely inaccessible or buried torus, because the entire inner surface of the torus is buried from contact with the solvent. The method for distinguishing between these two cases is discussed in Appendix I.

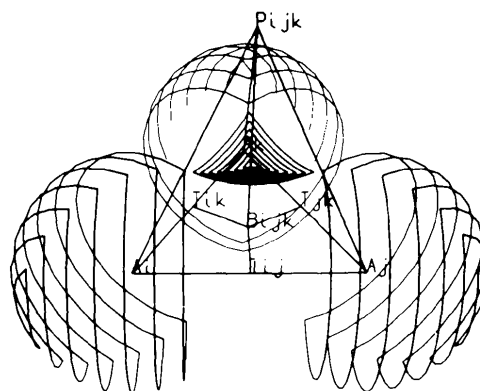


Fig. 6. Probe placement. The center of a probe sphere placed in contact with three atoms and the inward-facing part of the probe-sphere surface are shown. The probe center, tori centers, atom centers and base point are labeled.

For the situation where the quantity under the square root is positive, there are two probe positions. At this point, even before we check for collision, we know that none of the three tori, ij , ik or jk , can be free, and so they are each marked as being non-free tori. This information is important, because before the probe placement step all tori are initialized as being free, while, after this step is completed, all tori that remain marked free are given a continuous loop of saddle surface.

Each of the two probe positions must be checked for van der Waals overlap or collision with mutual neighbors of atoms i , j and k . The probe sphere and an atom collide if the separation of their centers is less than the sum of their radii.

For each probe placement that survives collision checks with neighboring atoms, a concave face is generated. The equations for the vertices of this spherical triangle are given in Table 2. The boundary arcs are parts of great circles on the probe sphere connecting these vertices. A great circle is a circle of maximum diameter lying on a sphere, so that the circle and sphere centers coincide.

Each of the three edges of the triangle bridges the van der Waals surfaces of a pair of atoms (ij , jk or ik) and each edge is appended to a list for the torus between that pair of atoms. This facilitates the retrieval of edges at the next stage, when saddle faces are constructed by connecting adjacent pairs of concave edges belonging to the same torus.

For later purposes of defining saddle and convex faces, it is useful to assign an orientation to each edge. An edge orientation says which vertex is the starting vertex and which vertex is the ending vertex of the arc. For each concave face, the three concave edges are oriented so that the face appears counter-clockwise when viewed from the probe-sphere center.

Each concave face is associated with three tori. There is no need to create the face three times, once each while considering a probe rolling around each of the three tori. Therefore, for the torus between atoms i and j , a mutual neighbor k is considered for probe placement only if $i < j < k$. However, it is still necessary to consider every mutual neighboring atom k for the check that it may render the entire torus inaccessible.

It is unusual for a single mutual neighbor to block completely a probe from simultaneously touching atoms i and j at any point around the inter-atomic axis. The more common situation is where several neighboring atoms collectively bury the torus. This situation is recognized by the fact that after the probe placement part of the algorithm is finished, some non-free tori will not be marked as having been buried by a single atom, but will, nonetheless, have empty edge lists. Since concave arcs are added to the edge list of a torus not only when that particular torus is being considered for probe placement, but also when the

probe is being placed around another torus where the two tori share an atom, then it is not possible to recognize the situation where a torus has an empty edge list until all tori about all pairs of atoms have been considered for probe placement.

Saddle faces

After all the concave edges have been generated and each assigned to the appropriate torus, each torus is examined to create saddle faces. Buried tori generate no surface. Free tori are considered as a special case. Their saddle faces have no concave edges, and their convex edges are complete contact circles (defined below).

For tori partially accessible to solvent, one or more saddle-shaped rectangles are formed. The concave edges are in the torus edge list in order of creation, but, for the purpose of forming saddle faces, they must be sorted into a new list so that this new list is in clockwise order when viewed along the torus axis from atom i to atom j . When two concave arcs are adjacent in space, and so may border the same saddle face, they are in adjacent elements in this new list. Whether an edge is paired with the edge before or the edge after is determined by the method of saddle-face orientation, described below.

The vertices of the concave edges lie on the two circles of contact between the torus and the atoms. The center and radius of the contact circle on atom i are given in Table 2. The contact circle on atom j is defined by the same formulas, but with i and j interchanged. The circles are given an orientation so that when looking along the torus axis from atom i to atom j , the circle on atom i is counter-clockwise, and the circle on atom j is clockwise.

A saddle face is constructed by choosing a pair of adjacent concave edges and the pair of convex arcs connecting them so that the orientation of the result-

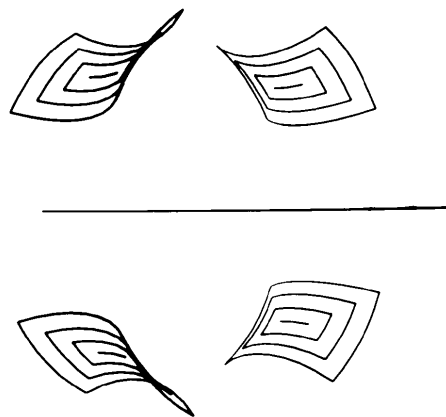


Fig. 7. Saddle-face construction. The accessible part of the inward-facing surface of the torus is made up of a disconnected set of saddle-shaped rectangles. The line represents the torus axis.

ing rectangle is clockwise when viewed from outside the molecule. The convex edges inherit the orientation of the circle they lie on. All concave edges are paired in this way to construct a disconnected set of saddle faces going around the torus axis (Fig. 7). Assigning orientations is a bookkeeping device that ensures that the saddle faces created are the regions accessible to a probe sphere, and not the gaps that they alternate with about the torus axis.

For each saddle face constructed, a pair of convex arcs is generated. Each convex arc is appended to the list of convex arcs for that atom. These convex arcs are used in the next step of convex-face generation.

Convex faces

Convex faces are generated for each partially or wholly accessible atom. Buried atoms generate no surface. Atoms whose entire surface is accessible are a special case. They have one convex face with no boundary. Both buried and completely accessible atoms have null edge lists, but they may be distinguished by the fact that completely accessible atoms have no neighbors. For partially accessible atoms, which have one or more convex edges, convex faces are generated as follows.

All the convex edges belonging to the edge list of the atom are grouped into cycles. An edge with no end points (a circle) forms a cycle by itself. Edges with end points form cycles where the second vertex of one edge is equal to the first vertex of the next edge, and so on, around the cycle, until the second vertex of the last edge of the cycle coincides with the first vertex of the first edge. Since the convex edges have an orientation, the cycles that result from linking them together also have an orientation.

This orientation is used to define the interior of the cycle. The interior of a cycle is the part of the van der Waals surface of the atom that lies on the left-hand side of the edges as one travels around the cycle in the direction of its orientation. The exterior lies on the right-hand side. The interior of a cycle is in general solvent-accessible, except for the case where other cycles are present in the interior, making part of the interior of this cycle solvent-excluded. Each cycle appears counter-clockwise when viewed from above its interior.

A convex face is defined by listing the cycles that form its boundary. So, once the cycles of an atom have been formed, it is necessary to partition the cycles into groups. All the cycles in a given group border a particular face. If two cycles border the same face, then they will lie in each other's interior. The first step in forming convex faces, then, is to compare every pair of cycles to determine whether the first lies in the interior of the second, and *vice versa* (Fig. 8).

We determine whether cycle *A* lies within the interior of cycle *B* as follows. Cycles do not intersect,

so we need check only one point *P* of cycle *A* in order to determine whether the whole of *A* lies in the interior of *B*. We arbitrarily choose the first vertex of the first edge as our point *P*, unless cycle *A* consists of a single circle with no vertices, in which case we choose the center of the exterior of this circle as our point *P*.

Stereographic projection of the sphere onto the plane (do Carmo, 1976) is used to determine whether the point *P* lies in the interior of cycle *B*. The point *P* is chosen as the north pole of the stereographic projection, and the vertices of cycle *B* are projected onto the plane tangent to the south pole of the atom (Fig. 9). The projected vertices are connected by straight lines to form a polygon, and the polygon edges are given the same orientation as the convex arcs they come from. If the point *P* lies inside the cycle, the polygon will have a counter-clockwise orientation, just like the cycle itself. If the point *P* lies outside the cycle, the projection will reverse the orientation so that the

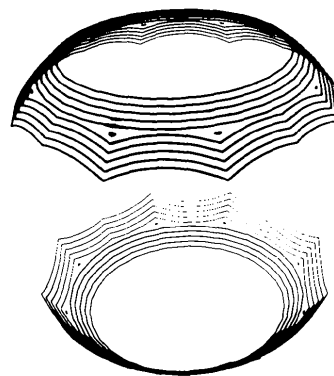


Fig. 8. Cycles. The atom has two regions of solvent-accessible van der Waals surface, each bordered by two cycles. The interior of each face is also represented by cycles. After the convex edges on the atom are grouped to form four cycles, the cycles must be grouped to form two faces.

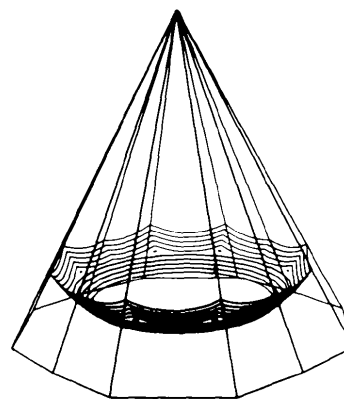


Fig. 9. Stereographic projection. The vertices of a boundary cycle are projected onto a plane tangent to the atom and opposite the origin of the projection.

polygon has a clockwise orientation. The orientation of the polygon is determined by the sign of the sum of its exterior angles. The arcs of the cycle do not project onto straight lines, but this is irrelevant, because the only property of the polygon that we are concerned with is its orientation.

There are two situations where stereographic projection is not necessary. If cycle *B* contains fewer than three arcs, then its exterior is completely blocked by the one or two neighboring atoms that generated these arcs, and so all other cycles, including *A*, must lie in the interior of cycle *B*. The other situation occurs when cycles *A* and *B* each have a convex edge belonging to the same torus, in which case it is clear that each cycle must lie in the other's exterior.

After every pair of cycles has been compared, and their relative interior/exterior relations stored, convex faces are formed. If two cycles border the same face, then each lies in the other's interior, but the converse is not necessarily true. In order for cycles *A* and *B* to border the same face, not only must they lie in each other's interior, but also every other cycle *C* that lies in the interior of cycles *A* and *B* must have both cycles *A* and *B* in its interior.

In this manner, the solvent-accessible van der Waals surface of the atom is divided into faces, each bordered by zero or more cycles of one or more arcs.

Self-intersecting surfaces

A saddle face intersects itself when the torus radius is less than the probe radius. It can also happen that two concave faces interpenetrate. These problems typically occur in deep grooves. Methods for dealing with these problems are being developed.

Area measurement

The area of each face of the surface may be measured once the surface has been calculated by the surface creation program. The output of the surface creation program is a list of convex, saddle-shaped and concave faces defined in terms of vertices, circular arcs, spheres and tori (Fig. 4), according to the equations given in Table 2. This output is used directly as input to the area measurement program.

Different area computation methods are used for each of the three types of faces. All methods have in common the fact that areas are defined in terms of the radii and angles presented in Table 2. The equations for the areas are given in Table 3 and derived below.

Concave face

The area of a concave face may be calculated from its angles (Fig. 10), since it is a spherical triangle (do Carmo, 1976).

$$A_{..} = r_p^2 \left(\sum_v \beta_v - \pi \right). \quad (1)$$

Table 3. *Molecular areas*

Face	Area
Convex	$A_{..} = r_i^2 \left[2\pi\chi - \sum_s \varphi_s \sin \theta_{si} - \sum_v (\pi - \alpha_v) \right]$
Saddle	$A_s = \varphi_s [r_{ij} r_p (\theta_{si} + \theta_{sj}) - r_p^2 (\sin \theta_{si} + \sin \theta_{sj})]$
Concave	$A_{..} = r_p^2 \left(\sum_v \beta_v - \pi \right)$

Saddle face

The area of a saddle face is calculated by integration (Fig. 11). The parts of the saddle surface on either side of the midline are integrated separately.

The area of the surface of revolution is calculated by integrating a strip of width $r_p d\theta$ and length $\varphi_s x$, where θ ranges from 0 to θ_{si} , and $x = r_{ij} - r_p \cos \theta$. The area of the part of the saddle next to atom *i* is given by

$$A_{si} = \int_0^{\theta_{si}} \varphi_s x r_p d\theta = \varphi_s r_p (r_{ij} \theta_{si} - r_p \sin \theta_{si}). \quad (2)$$

A similar term exists for the part of the saddle surface next to atom *j*, but with θ_{si} replaced by θ_{sj} . The

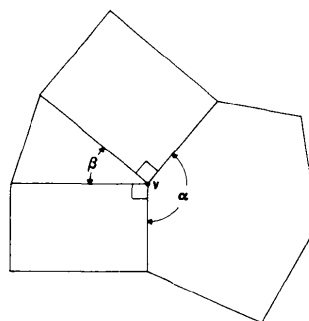


Fig. 10. Angles at a vertex. Two saddle rectangles, one concave triangle and one convex region meet at each vertex. The sum of the angles is 2π .

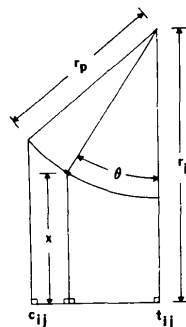


Fig. 11. Saddle-face-area computation. The angle θ varies between 0 at the midline and θ_{si} at the contact circle on atom *i*. The part of the saddle face next to atom *j* (not diagrammed) is integrated separately, with the angle θ varying between 0 and θ_{sj} . The distance of the element of area from the torus axis is denoted by *x*.

combined saddle surface area is then

$$A_s = A_{s_i} + A_{s_j} \\ = \varphi_s [r_i r_p (\theta_{s_i} + \theta_{s_j}) - r_p^2 (\sin \theta_{s_i} + \sin \theta_{s_j})]. \quad (3)$$

Convex face

The area of a convex face is calculated by applying the Gauss-Bonnet theorem (do Carmo, 1976):

$$\sum_v (\pi - \alpha_v) + \sum_e \int k_e dl + \int K dA = 2\pi\chi. \quad (4)$$

The sum in the first term is over the vertices of the boundary and the sum in the second term is over the edges of the boundary of the face. This theorem from differential geometry expresses the Euler characteristic, χ , in terms of point, line and area curvature. The Euler characteristic depends on the number of holes in the surface and is equal to 2 minus the number of cycles forming the boundary.

The point curvature of the face is the sum of the exterior angles at the vertices. The exterior angle at a vertex is the angle between the two tangent vectors to the arcs and is equal to π minus the interior angle α_v (Fig. 10).

The line curvature of the face is the sum of the integral over each edge of the geodesic curvature. The geodesic curvature, k_e , of edge e is constant along each arc, and equal to $(1/r_c)\sin \theta_{s_i}$, where r_c is the radius of the contact circle and θ_{s_i} is the saddle-width angle of the saddle face s bordering this convex edge on atom i (derivation given in Appendix III). The length of the arc is $r_c \varphi_s$, where φ_s is the angle by which the saddle face s wraps around the inter-atomic axis. When the geodesic curvature and arc length are multiplied to give the value of the line integral, the contact-circle-radius factors cancel and we are left with $\varphi_s \sin \theta_{s_i}$. Since each edge corresponds to a saddle face, we may change the summation index in the second term in (4) from e to s .

Since a sphere has constant curvature, the area-curvature integral is equal to the Gaussian curvature times the convex-face area (A_+). The Gaussian curvature is equal to the reciprocal of the square of the atom radius. Substitution of all the above information into (4) gives

$$\sum_v (\pi - \alpha_v) + \sum_s \varphi_s \sin \theta_{s_i} + \frac{1}{r_i^2} A_+ = 2\pi\chi. \quad (5)$$

Solving for the area we get

$$A_+ = r_i^2 \left[2\pi\chi - \sum_s \varphi_s \sin \theta_{s_i} - \sum_v (\pi - \alpha_v) \right]. \quad (6)$$

Two simple examples are considered. If the boundary of the convex face consists of a single circle, then the Euler characteristic is 1, the saddle wrap angle is 2π , and there are no vertices. The formula simplifies to $A_+ = 2\pi r_i^2 (1 - \sin \theta_{s_i})$. If the convex face consists of an

entire sphere, then the Euler characteristic is 2 and the other terms are zero, giving the familiar formula $A_+ = 4\pi r_i^2$.

A method for measuring the volume enclosed by the surface has been developed (Connolly, 1983c).

Computer graphics

The surface may be displayed on a vector computer-graphics system. This requires that the output of the surface generation program be processed by a subsequent program. Each face of the analytically-defined surface is converted into a set of concentric curved polygons (Fig. 3). The arcs of the polygons are drawn as a series of short vectors, since most vector graphics systems will draw only straight lines.

The construction of concentric polygons is straightforward for concave and saddle faces, but more complicated for convex faces. We consider each of these three cases.

Concave face

A point is chosen in the center of the concave triangle. This point is then connected to each of the three vertices by great circular arcs. Each of these three connecting arcs is subdivided by the same number of points. Corresponding triplets of subdivision points are connected by great circular arcs to form concentric triangles. The triangle corresponding to the boundary of the concave face is not drawn, to prevent overlapping drawing of concave and saddle faces.

Saddle face

The concave pair of arcs of the saddle face are subdivided by equally spaced points. Pairs of corresponding points are connected by convex arcs that lie in planes perpendicular to the torus axis. This rectangular subdivision could be drawn as a grid, but instead it is represented by concentric curved rectangles. The largest rectangle has its concave sides along the concave boundary arcs, but its convex sides are one subdivision in from the boundary, to prevent overlap with convex faces.

Convex face

Convex faces have less-regular shapes than concave and saddle faces. Both the number of cycles forming the boundary and the number of edges per cycle are variable. Simple subdivision algorithms, such as those described above for concave and saddle faces, will not work. A more general method is needed.

The basic idea in this more general method is to increment progressively the radii of atoms that neighbor a face in order to generate a series of shrinking contact areas. An atom neighbors a face if an edge of the face lies on the torus between the central atom and this neighbor.

The first step in this procedure is to gather all the atoms that neighbor the given face. Then a simplified version of the surface-creation algorithm is repeatedly applied to just this central atom and its neighbors. Before each application, the radii of neighboring atoms are incremented.

The size of the radius increment depends on both the step number and the neighbor, according to the following initialization and iteration equations.

$$\epsilon_0 = \arctan(r_c/d_c), \quad r_{j,0} = r_j \quad (7)$$

$$\epsilon_n = \epsilon_{n-1} + S/r_i \quad (8)$$

$$r_{j,n} = \{[d_{ij} - (r_i + r_p)\cos \epsilon_n]^2 + (r_i + r_p)^2 \sin^2 \epsilon_n\}^{1/2} - r_p \quad (9)$$

The value of S must be specified to give the distance separating successive polygons. The radius of atom j at step n is denoted by $r_{j,n}$. The angle ϵ_n is defined in Fig. 12. See Fig. 17 in Appendix I for r_c/d_c .

As the contact area shrinks, some neighbors may no longer contribute edges, so the number of sides of the polygon may decrease. It is also possible that a cycle may split into two or more cycles.

There are two conditions that signal when the contact area has gone to zero. One occurs when $\epsilon_n \geq \pi$ for some neighboring atom, which means that this neighboring atom has grown large enough to bury the central atom completely. The other event is the failure of an iteration to produce any convex edges, which means that the neighbors have grown large enough to bury collectively the central atom.

A special check ensures that all the convex edges produced lie in the interior of the original face, rather than in some other region of the atom. This check occurs in the probe-placement part of the algorithm, where the contact point between the probe and central atom is determined to lie inside or outside the original convex face, by the method of stereographic projection described above (Fig. 9). This point must lie in the interior of each cycle of the face, or else this probe position is discarded.

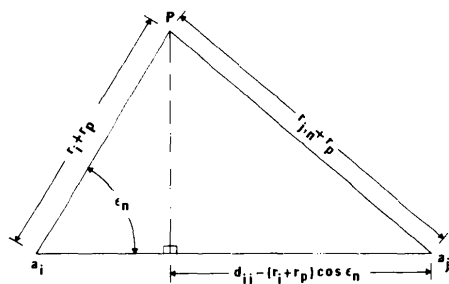


Fig. 12. Neighbor-atom-radius increment. The radius of the central atom (left) is fixed, but the radius of the neighbor on the right is incremented by an amount chosen so that the spacing of convex edges on the central atom will be the same for each step.

The arcs of the boundary cycles of the original face are drawn, in addition to the convex edges generated by the iterative procedure described above.

This surface representation may be displayed on an Evans and Sutherland Multi Picture System by using the general-purpose display program *GRAMPS* (O'Donnell & Olson, 1981).

A method for displaying an analytical molecular surface on a color raster terminal has been developed (Connolly, 1983b). This method does hidden-surface elimination and shading (Fig. 3). Scientific applications of the vector and raster graphics methods, molecular-area and volume-measurement methods, and the dot surfaces are discussed by Connolly (1983a).

I thank T. J. O'Donnell and A. J. Olson for the use of their program *GRAMPS*, the Brookhaven National Laboratory Protein Data Bank for X-ray coordinates (Bernstein *et al.*, 1977), and the Helen Hay Whitney Foundation for a postdoctoral fellowship.

APPENDIX I

Derivation of surface definition equations

The simple equations in Table 2 are not derived.

Torus

Consider a probe sphere placed tangent to two atoms, i and j . The triangle with the probe center as its vertex and the inter-atomic axis as its base may be divided into two right triangles, with the right angles meeting at the torus center (Fig. 13). The torus center will be halfway between the two atom centers only if they have the same radius.

Let the variable x denote the distance from the center of atom i to the torus center, so that $\mathbf{t}_{ij} = \mathbf{a}_i + x\mathbf{u}_{ij}$. The length of the other leg of the right triangle is the torus radius r_{ij} and the hypotenuse has length $r_i + r_p$, so we have

$$x^2 + r_{ij}^2 = (r_i + r_p)^2. \quad (A1)$$

There is a similar equation for the other right triangle:

$$(d_{ij} - x)^2 + r_{ij}^2 = (r_j + r_p)^2. \quad (A2)$$

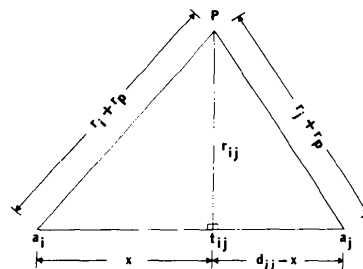


Fig. 13. Torus center and radius. The torus center will be closer to the smaller atom.

These are two equations in two unknowns, x and r_{ij} . Subtracting the second from the first and solving for x we get

$$x = \frac{1}{2}d_{ij} + \frac{1}{2}[(r_i + r_p)^2 - (r_j + r_p)^2]/d_{ij}. \quad (A3)$$

Substituting this value for x into $\mathbf{t}_{ij} = \mathbf{a}_i + x\mathbf{u}_{ij}$ and rearranging terms we get

$$\mathbf{t}_{ij} = \frac{1}{2}(\mathbf{a}_i + \mathbf{a}_j) + \frac{1}{2}(\mathbf{a}_j - \mathbf{a}_i)[(r_i + r_p)^2 - (r_j + r_p)^2]/d_{ij}^2. \quad (A4)$$

Substituting the value for x given in (A3) into (A1) and rearranging terms we get

$$r_{ij} = \frac{1}{2}[(r_i + r_j + 2r_p)^2 - d_{ij}^2]^{1/2}[d_{ij}^2 - (r_i - r_j)^2]^{1/2}/d_{ij}. \quad (A5)$$

Base point

The base point for a probe sitting on atoms i, j and k is located at the intersection of the three torus-bisecting planes and the base plane (Fig. 14). Let y denote the distance from the torus center \mathbf{t}_{ij} to the base point \mathbf{b}_{ijk} , so $\mathbf{b}_{ijk} = \mathbf{t}_{ij} + y\mathbf{u}_{tb}$.

The vectors from \mathbf{t}_{ij} to \mathbf{t}_{ik} and from \mathbf{t}_{ij} to \mathbf{b}_{ijk} both project onto the same vector on the ik axis. This gives us

$$\mathbf{u}_{ik} \cdot (\mathbf{t}_{ik} - \mathbf{t}_{ij}) = \mathbf{u}_{ik} \cdot (\mathbf{b}_{ijk} - \mathbf{t}_{ij}). \quad (A6)$$

The angle between \mathbf{u}_{ik} and $\mathbf{b}_{ijk} - \mathbf{t}_{ij}$ is equal to $\pi/2 - \omega_{ijk}$ and the length of the second vector is y , so (A6) may be written

$$\mathbf{u}_{ik} \cdot (\mathbf{t}_{ik} - \mathbf{t}_{ij}) = y \cos(\pi/2 - \omega_{ijk}) = y \sin \omega_{ijk}. \quad (A7)$$

Solving for y and substituting into $\mathbf{b}_{ijk} = \mathbf{t}_{ij} + y\mathbf{u}_{tb}$ we get

$$\mathbf{b}_{ijk} = \mathbf{t}_{ij} + \mathbf{u}_{tb}[\mathbf{u}_{ik} \cdot (\mathbf{t}_{ik} - \mathbf{t}_{ij})]/\sin \omega_{ijk}. \quad (A8)$$

Probe height

The right triangle between the center of atom i , the base point and the probe position (Fig. 15) has legs of

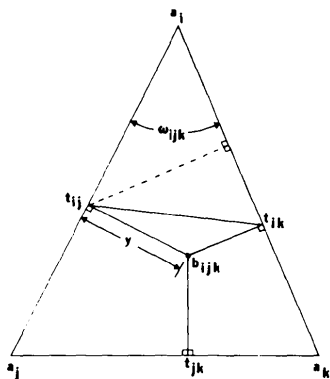


Fig. 14. Base point for probe positions. The center of a probe sphere touching the three atoms lies on a line perpendicular to the plane passing through the three atomic centers, and intersecting this plane at the base point \mathbf{b}_{ijk} .

length $|\mathbf{b}_{ijk} - \mathbf{a}_i|$ and h_{ijk} and the hypotenuse has length $r_i + r_p$. This gives

$$|\mathbf{b}_{ijk} - \mathbf{a}_i|^2 + h_{ijk}^2 = (r_i + r_p)^2. \quad (A9)$$

Solve for h_{ijk} :

$$h_{ijk} = [(r_i + r_p)^2 - |\mathbf{b}_{ijk} - \mathbf{a}_i|^2]^{1/2}. \quad (A10)$$

The probe height is imaginary in the case where the probe cannot be placed simultaneously tangent to all three atoms. This happens when the torus central circle does not intersect the sphere centered at atom k with radius $r_k + r_p$ (locus of centers of probes tangent to atom k). This may occur either because the torus central circle lies entirely outside the sphere, or because it lies entirely inside the sphere. In the second case the torus will be completely buried by atom k , because any probe placed tangent to atoms i and j will overlap atom k . These two cases may be distinguished by considering the distance between the torus center and atom k .

First we consider the special case where the center of atom k lies on the torus axis (Fig. 16). The circle will lie exactly on the sphere when

$$|\mathbf{t}_{ij} - \mathbf{a}_k| = [(r_k + r_p)^2 - r_{ij}^2]^{1/2}. \quad (A11)$$

When this distance $|\mathbf{t}_{ij} - \mathbf{a}_k|$ is less than the quantity on the right, then the torus central circle will lie entirely within the sphere. When it is greater, it will lie entirely outside.

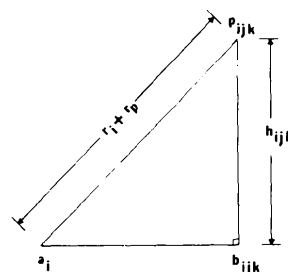


Fig. 15. Probe height above the base point.

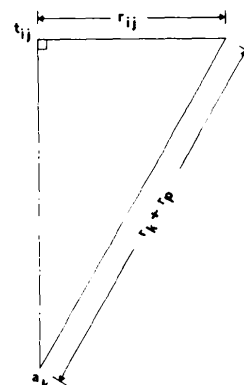


Fig. 16. Calculation of the distance between the torus center and atom k when the torus central circle lies exactly on the sphere centered at atom k with radius $r_k + r_p$.

In the more general case, where the torus plane is not perpendicular to the line joining the torus center and atom k , (A11) is still relevant. Since we are assuming that the circle does not intersect the sphere, a slanted circle must be even closer to a_k when it is entirely inside, or even farther from a_k when it is entirely outside the sphere. Therefore, we may make the general statement that when the probe height is imaginary, then the torus is completely buried by atom k if and only if

$$|\mathbf{t}_{ij} - \mathbf{a}_k| < [(r_k + r_p)^2 - r_{ij}^2]^{1/2}. \quad (\text{A12})$$

Contact circle

The center and radius of the contact circle and the vertex coordinates may be determined from the observation that the $\mathbf{a}_i \mathbf{c}_{ij} \mathbf{v}_{pi}$ and $\mathbf{a}_i \mathbf{t}_{ij} \mathbf{p}_{ijk}$ triangles are similar (Fig. 17).

APPENDIX II Numerical algorithm

The analytical algorithm is an outgrowth of an earlier numerical algorithm, which is described in this Appendix. This numerical algorithm generates a set of points lying on the same surface as the analytical algorithm calculates, but the faces and their boundary arcs are not explicitly computed. The points lying on convex, saddle and concave faces are each generated in their own way.

The points on convex faces are generated by placing a probe sphere tangent to a given atom at a finite number of positions. The positions are chosen along circles of latitude on the atom sphere. The spacing of the points along the latitudes and the spacing between the latitudes depends upon an input parameter. Each probe position is checked for van der Waals overlap with neighboring atoms. When there is no collision, the point of tangency between the probe and the atom is written to disk as a contact surface point.

The points on the saddle faces are created by placing a probe sphere tangent to a given pair of atoms. The center of the probe sphere is placed at a

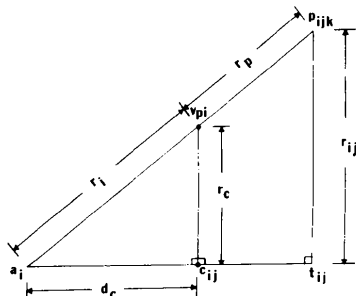


Fig. 17. Contact circle center and radius. The displacement of the contact circle from the atom center, d_c , is a signed quantity, being negative when the contact circle is on the opposite side of atom i from atom j .

finite number of positions along the torus central circle. Probe positions surviving collision checks with neighboring atoms generate surface points evenly spaced along the great circular arc on the probe sphere connecting the two points of contact. These arc points are written to disk as reentrant surface points.

The points on the concave faces are created by placing a probe sphere tangent to triples of atoms, in the same manner as in the analytical method. But, instead of representing the concave spherical triangle by its boundary arcs and vertices, a set of points lying within the triangle is written to disk as reentrant surface points. The points are chosen from a fixed set of points that are spaced along circles of latitude on the probe sphere.

The reentrant surface points are assigned to the atom whose van der Waals surface they are closest to. Each surface point, whether part of the contact or the reentrant surface, thus belongs to a particular atom. The display of these surface points on a vector graphics system having a dot-drawing mode is straightforward. This is in contrast to the situation for the analytical algorithm, where the more abstract representation must be converted by the concentric curved polygon program into a set of vectors.

The numerical algorithm produces not only the coordinates of a surface point, but also an outward-pointing unit vector perpendicular to the surface at that point, and an approximate area associated with the point.

APPENDIX III Geodesic curvature of a circle on a sphere

The geodesic curvature of a great circle is always zero. A small circle is a circle whose center does not necessarily coincide with the center of the sphere. The geodesic curvature of such a circle may be calculated by applying the Gauss-Bonnet formula [(4)] to a spherical cap. A spherical cap is a region on a sphere bounded by a circle. The area of a spherical cap is given by $A_{\text{cap}} = 2\pi r h$, where r is the radius of the sphere and h is the height of the cap (Gellert, Küstner, Hellwich & Kästner, 1975). This height may be expressed in terms of our variables as $r_i - d_c$, where r_i is the radius of atom i and d_c is the displacement of the contact-circle center from the atom center. So $A_{\text{cap}} = 2\pi r_i (r_i - d_c)$.

Applying (4) to this special case, we have 0 for the first term, because there are no vertices. The second term is the geodesic curvature times the circle circumference. The third term is the spherical-cap area times the Gaussian curvature (reciprocal of the atom-radius squared). The Euler characteristic of a spherical cap is 1. Substituting this information into (4), we get

$$k_c(2\pi r_c) + 2\pi r_i (r_i - d_c)/r_i^2 = 2\pi. \quad (\text{A13})$$

This equation may be solved for the geodesic curvature to give $k_e = d_c/(r_i r_c)$. Substitution of $\sin \theta_{si} = d_c/r_i$ gives $k_e = (1/r_c)\sin \theta_{si}$.

References

- ALDEN, C. J. & KIM, S.-H. (1979). *J. Mol. Biol.* **132**, 411–434.
- BERNSTEIN, F. C., KOETZLE, T. F., WILLIAMS, G. J. B., MEYER, E. F. JR, BRICE, M. D., RODGERS, J. R., KENNARD, O., SHIMANOCHI, T. & TASUMI, M. (1977). *J. Mol. Biol.* **112**, 535–542.
- CARMO, M. P. DO (1976). *Differential Geometry of Curves and Surfaces*, pp. 67, 264–283. Englewood Cliffs, New Jersey: Prentice-Hall.
- CONNOLLY, M. L. (1981a). Thesis, Univ. of California at Berkeley.
- CONNOLLY, M. L. (1981b). *Quantum Chem. Prog. Exchange Bull.* **1**, 75. The dot molecular surface program (MS) is written in Fortran and may be obtained by writing to: Quantum Chemistry Program Exchange, Department of Chemistry, Indiana University, Bloomington, Indiana 47405, USA.
- CONNOLLY, M. L. (1983a). *Science*. Accepted.
- CONNOLLY, M. L. (1983b). *Comput. Graphics*. Submitted.
- CONNOLLY, M. L. (1983c). *J. Am. Chem. Soc.* To be submitted.
- DODSON, E. J., DODSON, G. G., HODGKIN, D. C. & REYNOLDS, C. D. (1979). *Can. J. Biochem.* **57**, 469–479.
- FINNEY, J. L. (1978). *J. Mol. Biol.* **119**, 415–441.
- GELLERT, W., KÜSTNER, H., HELLWICH, M. & KÄSTNER, H. (1975). *The Van Nostrand-Reinhold Concise Encyclopedia of Mathematics*, pp. 198–200. New York: Van Nostrand-Reinhold.
- GREER, J. & BUSH, B. L. (1978). *Proc. Natl Acad. Sci. USA*, **75**, 303–307.
- LEE, B. & RICHARDS, F. M. (1971). *J. Mol. Biol.* **55**, 379–400.
- O'DONNELL, T. J. & OLSON, A. J. (1981). *Comput. Graphics*, **15**, 133–142.
- RICHARDS, F. M. (1977). *Ann. Rev. Biophys. Bioeng.* **6**, 151–176.
- RICHMOND, T. J. & RICHARDS, F. M. (1978). *J. Mol. Biol.* **119**, 537–555.